DELAYLESS SUBBAND ECHO CANCELERS USING COMPUTATIONALLY EFFICIENT PARALLEL KALMAN FILTERS

Mohammad Zulhasnine and Md. Kamrul Hasan

Department of Electrical and Electronic Engineering,
Bangladesh University of Engineering and Technology, Dhaka-1000, Bangladesh

ABSTRACT

Conventional delayless subband filters use LMS or NLMS algorithm for coefficient adaptations in subband domain. It is known that Kalman filter (KF) algorithm shows better convergence than the conventional LMS/NLMS algorithm but with the cost paid in computational complexity. In this work, we show that introducing parallel Kalman filters (PKFs) in the subband domain performance can be made better both in terms of ERLE and computational complexity than that of the LMS/NLMS algorithms.

1. INTRODUCTION

In recent years, adaptive filters are used in many applications such as adaptive modeling, adaptive noise cancellation, adaptive signal enhancement and adaptive echo cancellation [1], [2]. In some applications, such as acoustic echo cancellation and active noise control, where the number of filter taps to be estimated is large, computational complexity is a burden. Moreover, adaptive filters with many taps suffers from slow convergence, especially, if the eigenvalues of the underlying correlation matrix of the input signal are widely spread [2]. One approach for reducing the computational complexity of long adaptive filters is to use block signal processing methods [3]-[5]. The major disadvantage of such approaches is a long block delay associated with the adaptive weight update. The use of parallel Kalman filters (PKFs) in the time-domain is another approach for improving convergence rate [6].

Recently, subband techniques have been developed for adaptive filters to reduce the computational complexity and to improve the convergence rate [7]. As both the number of taps and weight update rate can be decimated in each subband, computational burden is reduced by approximately the number of subbands. Faster convergence is achieved due to the reduction of spectral dynamic range in each subband. The major disadvantages of subband structures, however, are aliasing due to downsampling [8] and the transmission delay introduced into the signal path due to the bandpass filters used for deriving the subband signals. To avoid signal path delay, Morgan and Thi reported a new type of subband adaptive filter architecture in which the adaptive weights are computed in subbands but collectively transformed into an equivalent set of wideband filter coefficients [9]. An additional benefit accrues through a significant reduction of aliasing effect. Commonly, subband implementations employ LMS or normalised LMS (NLMS) algorithm for its coefficients adaptation in each subband [3]-[5], [7]-[9]. Although the estimation algorithm of adaptive filters using such a method is simple, they are weak for the case of nonwhite input signal [6].

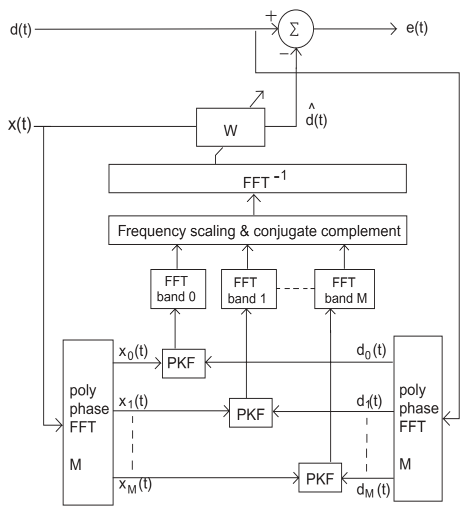

Fig. 1. Delayless subband parallel Kalman filter architecture.

In this paper, we modify the delayless subband adaptive filter [9] by replacing the conventional NLMS/KF algorithm with PKFs for coefficients adaptation in each subband. Incorporation of parallel architecture in each subband provides a flexibility in trade-off between the number of subbands and parallel filters in each subband for optimum performance of subband adaptive filters. A design method for PKFs in the subband domain is proposed. Computational complexity and experimental results comparing the performance of such adaptive subband parallel NLMS (PNLMS) and PKFs are shown.

2. DELAYLESS SUBBAND PARALLEL KALMAN FILTERS

Fig. 1 shows the architecture of the subband adaptive filter with PKFs. The reference signal $x(t)$ is filtered by W to cancel out the disturbance signal $d(t)$. The objective is to adjust the coefficients of the wideband filter W in order to minimize the local error in a mean square sense [9]. The wideband error is expressed as

$$e(t) = d(t) - \boldsymbol{w}^T(t)\boldsymbol{x}(t), t = 0, 1, 2, ... \quad (1)$$

where $\boldsymbol{x}(t) \equiv [x(t), x(t-1), ..., x(t-N+1)]^T$ is a vector comprising the N most recent reference samples, the superscript T denotes the transpose operation, and $\boldsymbol{w}(t)$ is a vector of length N wideband weights.

2.1. Subband Decomposition of Signals

There are several ways to derive complex subband signals employing polyphase FFT techniques [10]-[11]. In this paper, the reference signal $x(t)$, and the disturbance signal $d(t)$ are divided into several subband signals by using a polyphase FFT technique described in [10]. This technique realizes M contiguous single-sideband bandpass filters with their outputs downsampled by a factor $D = M/2$ to produce M complex subband signals. Also no band shifting is necessary due to regular structure; even subbands are centered at dc while odd subbands are centered at one half of the decimated sampling frequency [9]. Since for real signals, the wideband filter coefficient are real, only half of the subbands need to be processed. The m-th subband reference signal is mathematically expressed as

$$\begin{aligned} x_m(t) &= \sum_{k=0}^{K-1} a_k e^{\frac{j2\pi mk}{M}} x(t-k) && (2) \\ &= \sum_{n=0}^{M-1} e^{\frac{j2\pi mn}{M}} \sum_{l=0}^{L-1} a_{n+l} x(t-k) && (3) \end{aligned}$$

where a_k are the coefficients of a K point prototype filter and $K = LM$, L is a integer. It is obvious that Eq. (2) expresses the convolution of the frequency-shifted prototype filter with the filtered reference signal to obtain a single sideband reference signal. And the expression in Eq. (3) shows how the inverse FFT comes into play. The signal $d(t)$ is also decomposed in the similar way to obtain $d_m(t)$ corresponding to the m-th subband.

2.2. Configuration of Parallel Kalman Filters

In this paper, adaptive weights are computed in the subband domain using the complex PKF algorithm and then collectively transformed into frequency domain using the FFT, appropriately stacked, and inverse transformed to obtain the wideband filter coefficients, thereby eliminating any delay associated with the cancellation signal. For N wideband adaptive weights and a decimation factor D, there are N/D adaptive weights for each subband. Let $\boldsymbol{w}_m$ is a vector of N/D subband weights, $\boldsymbol{x}_m(t) \equiv [x(t), x(t-D), ..., x(t-N+D)]^T$ is a vector comprising the N/D most recent signals of the subband filter reference signal. Each subband signal is split into J segments for coefficients adaptation using the PKF algorithm as shown in Fig. 2 for the m-th subband. The adaptive weights of each subband are divided into J parts, namely Part 1, Part 2,..., Part J. As an example, the m-th subband FIR adaptive filter weights $\boldsymbol{w}_m$ in the z-domain can be represented as

$$W_m(z) = \sum_{i=0}^{N/D-1} w_{(m,i)} z^{-i} \quad (4)$$

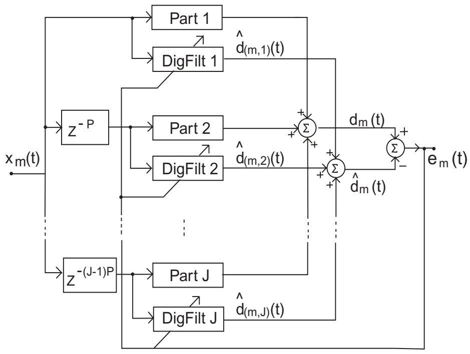

Fig. 2. Configuration of parallel Kalman filter of m-th subband.

If we divide the adaptive weights of the m-th subband $\boldsymbol{w}_m = [w_{(m,0)}, w_{(m,1)}, ..., w_{(m,N/D-1)}]^T$ into J parts, then $\boldsymbol{w}_m$ can be expressed as

$$\boldsymbol{w}_m = [\boldsymbol{w}_{(m,1)}^T, \boldsymbol{w}_{(m,2)}^T, ..., \boldsymbol{w}_{(m,J)}^T]^T \quad (5)$$

The adaptive weights of each part of the m-th subband are given by

$$\boldsymbol{w}_{(m,i)} = [w_{(m,P(i-1))}, w_{(m,P(i-1)+1)} ..., w_{(m,Pi-1)}]^T, \quad i = 1, 2, ..., J \quad (6)$$

where $P = N/(JD)$ is the number of elements of each part and J denotes the number of division in each subband. In Eq. (6), $w_{(m,P(i-1))}$ denotes the $P*(i-1)$-th coefficient of the m-th subband. If necessary some zeros should be added to the J-th part of the adaptive weights so as to make $P = N/(JD)$ an integer.

We divide the m-th subband signal $\boldsymbol{x}_m(t)$ into J parts expressed as

$$\boldsymbol{x}_m(t) = [\boldsymbol{x}_{(m,1)}^T(t), \boldsymbol{x}_{(m,2)}^T(t), ..., \boldsymbol{x}_{(m,J)}^T(t)]^T \quad (7)$$

Here, $\boldsymbol{x}_{(m,i)}(t)$ represents the m-th subband signals of the i-th part defined as

$$\begin{aligned} \boldsymbol{x}_{(m,i)}(t) = [&x_m(t - P(i-1)D), \\ &x_m(t - (P(i-1)D + D)), .. \\ &.., x_m(t - (P(i-1)D + JD))] \end{aligned} \quad (8)$$

The J segments of the impulse response described in Eq. (6) are estimated using J number of parallel filters. The total output of the J pieces of the filters in parallel is given by

$$\widehat{d}_m(t) = \sum_{i=1}^{J} \widehat{d}_{(m,i)}(t) = \sum_{i=1}^{J} \widehat{\boldsymbol{w}}_{(m,i)}^H(t-1)\boldsymbol{x}_{(m,i)}(t) \quad (9)$$

where $\widehat{d}_m(t)$ is the estimated subband disturbance signal at time t, and $\boldsymbol{w}_{(m,i)}(t)$ denotes the estimated weight vector. Notice that the order of the resultant filter in each subband is JP.

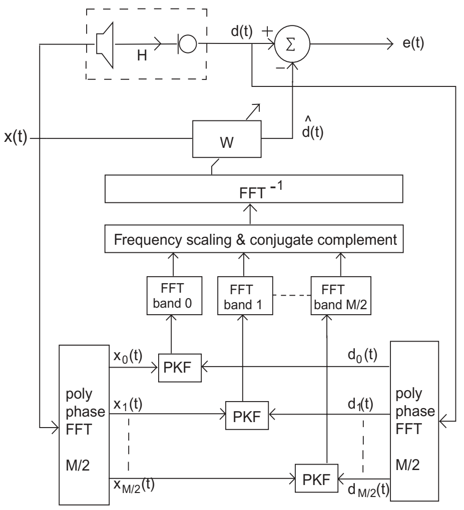

Fig. 3. Delayless subband adaptive parallel Kalman filter echo canceler.

2.3. Estimation Algorithm of the Parallel Kalman Filters

To obtain the optimal solution of the coefficients of the resultant filter, the subband total error $e_m(t) = d_m(t) - \widehat{d}_m(t)$ is used to estimate the parameters. The optimal algorithm for the i-th part in the m-th subband is obtained as shown in the following:

$$\widehat{\boldsymbol{w}}_{(m,i)}(t) = \widehat{\boldsymbol{w}}_{(m,i)}(t-1) + \boldsymbol{k}_{(m,i)}(t)e_m^*(t) \tag{10}$$

$$e_m(t) = d_m(t) - \widehat{d}_m(t) \tag{11}$$

$$\boldsymbol{k}_{(m,i)}(t) = \frac{\boldsymbol{Q}_{(m,i)}(t-1)\boldsymbol{x}_{(m,i)}(t)}{\lambda + \sum_{l=1}^{J} \boldsymbol{x}_{(m,l)}^H(t)\boldsymbol{Q}_{(m,l)}(t-1)\boldsymbol{x}_{(m,l)}(t)} \tag{12}$$

$$\boldsymbol{Q}_{(m,i)}(t) = [\boldsymbol{I} - \boldsymbol{k}_{(m,i)}(t)\boldsymbol{x}_{(m,l)}^H(t)]\boldsymbol{Q}_{(m,i)}(t-1) \tag{13}$$
$$i = 1, 2, ..., J; \quad t = D, 2D, 3D.....$$

$$\boldsymbol{Q}_{(m,i)}(0) = \beta_{(m,i)}\boldsymbol{I}; \beta_{(m,i)} > 0 \tag{14}$$

$$\widehat{\boldsymbol{w}}_{(m,i)}(0) = \boldsymbol{0} \tag{15}$$

where $\lambda = E\{e_m(t)e_m^*(t)\}$ and $\boldsymbol{I}$ is the unit matrix of dimension $M \times M$. The superscript $'*'$ denotes complex conjugation and the H indicates Hermitian transposition.

3. ACOUSTIC ECHO CANCELLATION

The acoustic echo canceler has been implemented using the proposed subband PKF algorithm as shown in Fig. 3. This is an open-loop echo canceler configuration where $x(t)$ is interpreted as the far-end received signal which drives the loudspeaker, H is acoustic echo path transfer function to the microphone signal $d(t)$, and $e(t)$ is the de-echoed returned signal (to which the desired signal is added). The assumed length (N) of the acoustic echo path is 2048. To decompose the signals into 16, 32, and 64 subbands; we use the MATLAB fir1(63,1/16), fir1(127,1/32), fir1(255,1/64) routine respectively. As the polyphase FFT implementation is assumed, only $M/2+1$ subband signals are estimated in all cases. The subband adaptive weights are transformed by 16/32/64-point (complex) FFT to obtain 16/32/64 frequencies per subband respectively, which are then properly stacked.

4. COMPUTATIONAL COMPLEXITY

Here, computational complexity is calculated based on the number of multipliers per input samples, assuming that the product of complex values is implemented through 4 real multiplies.

For M subbands, the $2\times$ oversampled subband decomposition [10] requires one convolution of a K-length prototype filter and and one M-point real FFT for each block of $M/2$ input samples. Therefore, the subband decomposition requires

$$C_1 = 2K/M + 2\log_2 M \tag{16}$$

real multiplies per input sample.

Since only half of the M complex subband signals are processed and subband filters are downsampled by a factor $D = M/2$, each of the $M/2$ lower subbands has to update $2N/M$ complex adaptive weights for each block of $M/2$ input samples. For close-loop version, with LMS/NLMS or parallel LMS/NLMS algorithm this requires

$$C_2 = 8N/(p_s * M) \tag{17}$$

real multiplies per input sample. Here p_s denotes the number of parallel section in each subband. For KF or PKF, the value of C_2 is given by

$$C_2 = 8(2N/(p_s * M))^2 + 16(2N/(p_s * M)) \tag{18}$$

For open-loop version, an additional C_2 real multiplies per input sample are required to evaluate the subband signal path convolutions. The subband-to-wideband filters mapping requires a $2N/M$-point complex FFT for each of the $M/2$ lower subbands and an N-point inverse real FFT. An $2N/M$-point complex FFT requires about $4N/M\log_2(2N/M)$ real multiplies. In practice, the wideband weights transformations are performed every N/J input samples, because the wideband filter output cannot change much faster than the length of its impulse response [9]. Typical value of J is in the range one to eight. This part thus requires

$$C_3 = [2\log_2(2N/M) + \log_2 N]J \tag{19}$$

real multiplies per input sample.

The wideband convolution is performed by partitioning the wideband filter into p segments. The number of multiplies per input sample is given by

$$\begin{aligned} C_4 &= N_p + 2p\log_2(2N_p) + 4(p-1) + 2\log_2(2N_p) \\ &= N/p + 2(p+1)\log_2(2N/p) + 4(p-1) \end{aligned} \tag{20}$$

Table 1. Comparison of computational complexity

No. of subband (M)	No. of parallel sections per subband	LMS algorithm		Kalman algorithm	
		C	ERLE	C	ERLE
64	1	1001	14.74	17897	22.80
16	4	1001	9.23	17897	22.69
64	8	553	7.51	873	18.83

considering that the product of complex values is implemented through 4 real multiplies. Here $N_p = N/p$ and the value of p is optimized so that the complexity over the direct convolution is optimized. Thus the total number of real multiplications required for the echo canceler is

$$C = C_1 + 2C_2 + C_3 + C_4 \tag{21}$$

As a comparison, it is to be noted that the computational complexity of the fullband LMS algorithm is approximately $2N$ and that of fullband Kalman filter is $8N^2 + 16N$ [6].

5. SIMULATION RESULTS

To evaluate the modified algorithm, we present computer simulation results. For comparison among different algorithms, consider the design of an $N = 2048$ tap real wideband echo canceler. Fig. 4 shows ERLE obtained for different algorithms namely NLMS, PNLMS, KF and PKFs. As expected, with equal number of subbands, KF/PKFs show better results than the conventional NLMS/PNLMS filter. The number of real multiplications required and ERLE obtained after 3000 iterations for each adaptive scheme are calculated and summarized in Table 1. The computational complexity is very large for KF than that of NLMS/PNLMS. But computational complexity drastically reduces for PKFs. As for example, with $M = 64$ and $p_s = 1$, ERLE obtained and number of real multiplies required for NLMS are 1001 and 14.74 and that for KF are 17897 and 22.08, respectively. Whereas, with $M = 64$ and $p_s = 8$, ERLE obtained and number of real multiplies required for PKFs are 873 and 18.83, respectively. Thus it is clear that PKFs show better results in terms of both ERLE and computational complexity when optimal number of parallel sections are incorporated in each subband. Moreover, the computational complexity of PKFs is comparable with that of PNLMS with much better ERLE index.

6. CONCLUSION

In this paper, we have designed an echo canceler in the delayless subband structure where coefficients of the filters are estimated using PKFs and PNLMS. Although KF in the subband domain yields improved convergence rate over NLMS/PNLMS filters, the cost paid to computational complexity is too high. But for our proposed PKFs in the subband domain computational complexity drastically reduces. In addition, PKFs maintain better convergence rate than that of NLMS/PNLMS. Thus the echo canceler employing PKFs in the subband domain offers computational savings, as well as faster convergence over that of NLMS/PNLMS filters.

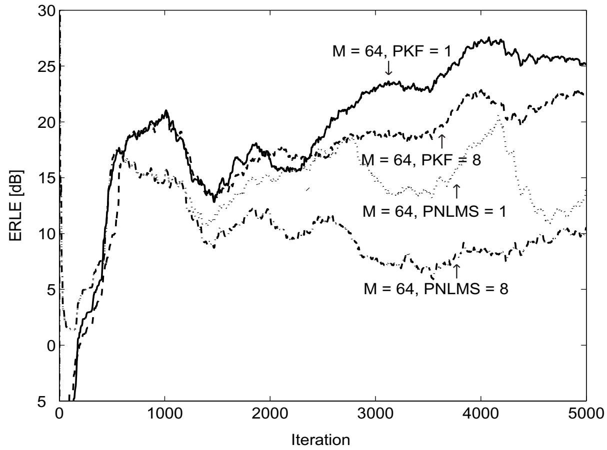

Fig. 4. ERLE obtained by different algorithms.

7. REFERENCES

[1] P. Diniz, "Adaptive Filtering: Algorithms and Practical Implementation," Boston, MA: Kluwer Academic, 1997.

[2] B. Widrow and S. D. Steams, "Adaptive Signal Processing," Prentice-Hall, Englewood Cliffs, NJ, 1985.

[3] G. A. Clark, S. K. Mitra, and S. R. Parker, "Block implementation of adaptive digital filters," *IEEE Trans. Circuits Syst.*, vol. CAS-28, pp. 584.592, 1981.

[4] J. M. Cioffi, J. A. C. Bingham, "A data-driven multitone echo canceler," *Proc. IEEE GLOBECOM '91*, pp. 2.4.1-2.4.5, 1991.

[5] Merched and A. H. Sayed, "An embedding approach to frequency-domain and subband adaptive filtering," *IEEE Trans. Signal Processing*, vol. 48, no. 9, pp. 2607-2619, 2000.

[6] J. Cao, T. Yahagi and J. Lu, "Parallel adaptive infinite impulse response digital filters" *Electronics and Communications in Japan.*, Part 3, vol. 78, no. 2., 1995.

[7] J. J. Shynk, "Frequency-domain and multirate signal processing," *IEEE Signal Processing Mag.*, vol. 9, pp. 14-37, 1992.

[8] A. Gilloire and M. Vetterli, "Adaptive fltering in subbands with critical sampling: Analysis, experiments, and application to acoustic echo cancellation," *IEEE Trans. Signal Processing*, vol. 40, no. 8, 1862-1875, 1992.

[9] D. R. Morgan, J. C. Thi, "A delayless subband adaptive filter architecture", *IEEE Trans. Signal Processing.*, vol. 43, no. 8., pp. 1819-1830, 1995.

[10] E. R. Ferrara Jr., "Frequency-domain adaptive filtering" in *Adaptive filters*, C. F. N. Cowan and P. M. Grant, Eds. Englewood Cliffs, NJ: Prentice Hall, 1985, chap 6, pp. 145-179.

[11] G. Wackersreuther, "Some new aspects of filter banks," *IEEE Trans. Acoust., Speech, Signal Processing.*, vol. ASSP-34, pp. 1182-1200, 1986.